Radioiodide imaging and radiovirotherapy of multiple myeloma using VSV(Δ51)-NIS, an attenuated vesicular stomatitis virus encoding the sodium iodide symporter gene

Apollina Goel,[1] Stephanie K. Carlson,[1,2] Kelly L. Classic,[3] Suzanne Greiner,[1] Shruthi Naik,[1] Anthony T. Power,[4] John C. Bell,[4] and Stephen J. Russell[1]

[1]Molecular Medicine Program, [2]Division of Radiation Oncology, Department of Radiology, [3]Section of Safety, Mayo Clinic College of Medicine, Rochester, MN; and [4]Ottawa Health Research Institute, University of Ottawa, Canada

Multiple myeloma is a radiosensitive malignancy that is currently incurable. Here, we generated a novel recombinant vesicular stomatitis virus [VSV(Δ51)-NIS] that has a deletion of methionine 51 in the matrix protein and expresses the human sodium iodide symporter (NIS) gene. VSV(Δ51)-NIS showed specific oncolytic activity against myeloma cell lines and primary myeloma cells and was able to replicate to high titers in myeloma cells in vitro. Iodide uptake assays showed accumulation of radioactive iodide in VSV(Δ51)-NIS–infected myeloma cells that was specific to the function of the NIS transgene. In bg/nd/xid mice with established subcutaneous myeloma tumors, administration of VSV(Δ51)-NIS resulted in high intratumoral virus replication and tumor regression. VSV-associated neurotoxicity was not observed. Intratumoral spread of the infection was monitored noninvasively by serial gamma camera imaging of ^{123}I-iodide biodistribution. Dosimetry calculations based on these images pointed to the feasibility of combination radiovirotherapy with VSV(Δ51)-NIS plus ^{131}I. Immunocompetent mice with syngeneic 5TGM1 myeloma tumors (either subcutaneous or orthotopic) showed significant enhancements of tumor regression and survival when VSV(Δ51)-NIS was combined with ^{131}I. These results show that VSV(Δ51)-NIS is a safe oncolytic agent with significant therapeutic potential in multiple myeloma. (Blood. 2007;110:2342-2350)

Introduction

Multiple myeloma is a malignancy of antibody-secreting plasma cells that reside predominantly in bone and bone marrow and secrete a monoclonal immunoglobulin.[1] The disease responds initially to alkylating agents, corticosteroids, and thalidomide, but eventually becomes refractory.[2] Multiple myeloma remains incurable causing more than 10 000 deaths each year in the United States.[3] Although cultured myeloma cells are relatively resistant to radiotherapy in vitro,[4,5] the malignancy is highly radiosensitive and radiation therapy is routinely used for palliation of pain, neurologic compromise, or structural instability from focal myeloma deposits. Efforts to use radiation as a systemic modality for definitive therapy of myeloma, however, have been problematic because of collateral toxicity to normal tissues especially the bone marrow progenitor cells.[6,7] Developing novel therapies for multiple myeloma based on the targeted delivery of radioisotopes to sites of active disease may have important clinical implications for myeloma therapy.

Gene transfer using the thyroidal sodium iodide symporter (NIS) gene offers a novel strategy for delivery of radionuclides to disseminated cancer cells.[8] NIS is a transmembrane protein in thyroid follicular cells that actively mediates iodide uptake to a concentration gradient more than 20 to 40-fold.[9] Cloning the human NIS cDNA has aided in imaging and therapy of dedifferentiated thyroid cancer and nonthyroid cancers such as glioma, neuroblastoma, melanoma, multiple myeloma, and ovarian, breast, cervix, lung, liver, and colon carcinoma.[10] Tissue-specific NIS expression has been achieved in various cancer xenografts with minimal toxicity to normal organs by using promoters and enhancers from genes encoding immunoglobulins, prostate-specific antigen, probasin, and mucin-1.[11-16]

Cancer therapy using oncolytic viruses (oncolytic virotherapy) requires agents that amplify efficiently through replication and spread causing rapid tumor lysis, yet are safe causing minimal toxicity to normal tissue enabling systemic inoculations to treat metastatic cancers.[17,18] We previously engineered the NIS gene into a lymphotropic, replication-competent attenuated strain of measles virus (MV-NIS)[19] that was subsequently used for oncolytic virotherapy of myeloma xenografts. Intratumoral spread of MV-NIS could be monitored noninvasively by radioiodine imaging and virus-resistant tumors were ablated after administration of ^{131}I.[20] A phase I clinical trial to evaluate the targeting properties of MV-NIS in patients with recurrent or refractory myeloma is ongoing at our institution. Several RNA viruses other than measles virus, including reovirus, Newcastle disease virus, mumps virus, and vesicular stomatitis virus (VSV), are being developed as systemic oncolytic agents for cancer therapy.[18,21] Each of these viruses has its own distinct cell-targeting mechanism and each one kills tumor cells by a different mechanism and with different kinetics. VSV is a negative-strand RNA virus classified under the family Rhabdoviridae, group vesiculoviruses, that has shown some promise as an antimyeloma agent in published preclinical studies.[22,23] VSV(Δ51) is an engineered mutant of VSV in which residue 51 of the matrix

Submitted January 3, 2007; accepted May 10, 2007. Prepublished online as *Blood* First Edition paper, May 21, 2007; DOI 10.1182/blood-2007-01-065573.

The publication costs of this article were defrayed in part by page charge payment. Therefore, and solely to indicate this fact, this article is hereby marked "advertisement" in accordance with 18 USC section 1734.

protein is deleted such that the matrix protein can no longer block the nuclear export of interferon-coding mRNAs. VSV(Δ51) therefore induces the expression of alpha/beta interferons (IFN-α/β), which prevent the infection from spreading in normal cells, but not in cancer cells.[24-26]

In the present study, we generated and characterized a novel oncolytic virus, VSV(Δ51)-NIS. The growth kinetics, oncolytic ability, and virus-encoded NIS transgene function were evaluated in vitro in myeloma cell lines and in primary samples from myeloma patients. In vivo studies used the 5TGM1 murine myeloma cell line, a variant of 5T33MM that originated spontaneously in aging C57BL/KaLwRij mice.[27] Both intratumoral and intravenous administrations of VSV(Δ51)-NIS showed pronounced oncolytic activity in bg/nd/xid mice bearing subcutaneous 5TGM1 myeloma tumors. Intratumoral spread of the VSV(Δ51)-NIS infection could be noninvasively and serially imaged by planar radioiodine scintigraphy and the data used for dosimetric calculations. In the syngeneic 5TGM1 model, regression of subcutaneous tumors was achieved in immunocompetent mice by intratumoral or intravenous administration of VSV(Δ51)-NIS, and the potency of this treatment could be further enhanced by subsequent administration of iodine-131 (^{131}I). Improved survival was also achieved in immunocompetent mice bearing orthotopic 5TGM1 myeloma tumors after radiovirotherapy. Based on its safety, oncolytic potency, and the feasibility of NIS-mediated radioiodine imaging and radiovirotherapy in multiple myeloma models, we believe that VSV(Δ51)-NIS is a promising experimental agent for the treatment of this disease.

Materials and methods

Cells

Myeloma cell lines were obtained from the American Type Culture Collection (MPC-11, CCL-167; ATCC, Manassas, VA), or were from Dr Rafael Fonseca (JJN-3, MM1) or Dr Diane Jelinek (RPMI 8226, KAS 6/1) at the Mayo Clinic (Rochester, MN). These were grown in RPMI 1640 supplemented with heat-inactivated 10% fetal bovine serum, 100 U/mL penicillin, and 100 mg/mL streptomycin; KAS 6/1 cells were supplemented with interleukin-6 (IL-6, 1 ng/mL). The 5TGM1 murine myeloma cell line (Dr Babatunde O. Oyajobi, University of Texas Health Science Center at San Antonio, TX) was grown in Iscove-modified Dulbecco media with 10% fetal bovine serum and penicillin-streptomycin antibiotics. African green monkey kidney cells (CCL-81, Vero) and mouse bone marrow stromal cells (SR-4987, CRL-2028) from ATCC were maintained in Dulbecco-modified Eagle medium containing 10% fetal bovine serum. Normal human skin fibroblasts (GM-5659D) were from the Coriell Institute for Medical Research (Camden, NJ). Primary cells ($CD138^+$ myeloma cells and $CD138^-$ or normal bone marrow progenitor cells) were obtained from the bone marrow of patients with advanced myeloma disease.[5] All tissue culture reagents were purchased from Gibco BRL (Rockville, MD).

Viruses

Polymerase chain amplification of human NIS has been described before.[20] VSV(Δ51)-NIS was generated using the established method of reverse genetics.[28] Briefly, the VSV(Δ51)-NIS genome was constructed by subcloning NIS cDNA into a plasmid encoding VSV(Δ51) at *Xho*I/*Nhe*I restriction sites within an extra cistron between the G and L genes.[26] This plasmid was used to rescue a recombinant VSV(Δ51)-NIS virus as described previously.[28] VSV(Δ51)–green fluorescent protein (GFP) contains an extra cistron-encoding GFP inserted between the G and L sequences.[29] VSV-GFP (Indiana strain)[29] was provided by Dr Glen N. Barber, University of Miami School of Medicine, Miami, Florida.

For amplification of recombinant VSVs (rVSVs), Vero cells were plated at a density of 1.5×10^6 cells/flask. Cells were infected the next day at a multiplicity of infection (MOI) of 0.01 for 1 hour. Virus was then removed and cells were incubated at 37°C in a CO_2 incubator until complete virus-induced cytopathic effect were seen. Culture medium was harvested, subjected to low-speed centrifugation, and filtered through a 0.45-μM filter. The supernatant was loaded on top of sucrose (10% w/v) and centrifuged at 70 000*g* for 2 hours to pellet the particles. For virus titration, Vero cells were grown on 96-well plates (7×10^3 cells/well/0.05 mL) and infected with 0.05 mL of serially diluted virus stock. Cells were incubated at 37°C in a CO_2 incubator. Tissue culture infectious dose $(TCID)_{50}$ values were determined by the Spearman and Karber equation: Log10 ($TCID_{50}$/mL) = L + d (s − 0.5) + log10 (1/v) as described before.[30] Virus stocks were stored at −80°C.

In vitro cytotoxic activity

Cytotoxicity of VSV(Δ51)-NIS on human and mouse myeloma cell lines was measured using the standard method of MTT [3-(4,5-dimethylthiazolyl-2)-2,-5-diphenyltetrazolium bromide] assay as described before.[5,31] Briefly, cells were mock-infected or infected with VSV(Δ51)-NIS (MOI = 1.0, 30 minutes at 37°C), unabsorbed virus was washed out, and cells were seeded into 96-well microplates at 10^4 cells per well in 0.1 mL medium. Plates were incubated for 24 or 48 hours, followed by the addition of .01 mL of MTT to each well. The mixture was incubated for 3 hours at 37°C. Formazan was extracted from the cells with 0.1 mL detergent and the color intensity was measured with a microplate enzyme-linked immunosorbent assay reader. Experiments were performed in triplicate. Results were recorded as percentage absorbance relative to untreated control cells and used to calculate cell death by VSV(Δ51)-NIS.

In vitro ^{125}I uptake studies

Iodide uptake studies were performed as described before.[20] Cells (5TGM1 or Vero; 1.5×10^5 cells/well) were plated into 12-well plates. The next day, cells were washed and incubated in serum-free Dulbecco-modified Eagle medium with VSV(Δ51)-NIS at an MOI of 1.0. After 30 minutes of incubation at 37°C, cells were washed and the medium was replaced with complete Iscove-modified Dulbecco media (5TGM1) or complete Dulbecco-modified Eagle medium (Vero) and incubated at 37°C for 48 hours before ^{125}I uptake. Cells were washed with Hanks balanced salt solution containing 10 mM HEPES [4-(2-hydroxyethyl)-1-piperazineethanesulfonic acid]. All wells, including the mock-infected wells, were incubated with an activity of 10^5 counts per minute (cpm) sodium-125 (Na^{125}) I/0.1 mL in 1 mL Hanks balanced salt solution containing HEPES. In controls, 100 μM $KClO_4$ was added to inhibit NIS-mediated iodide influx. Plates were incubated at 37°C for 45 minutes and then transferred to ice to inhibit the efflux after removal of I^- from the medium. Cells were washed twice with ice-cold Hanks balanced salt solution containing HEPES buffer. Cells were lysed with 1 M NaOH and the activity in the lysis buffer was determined by gamma counting. All data points were measured in triplicate and displayed as means plus or minus the SEM.

In vivo experiments

Animal studies were approved by the Animal Care and Use Committee, Mayo Clinic. Beige/nude/X-linked immunodeficient (bg/nd/xid, NIH background) mice at 5 to 8 weeks of age were purchased from Harlan Sprague Dawley (Indianapolis, IN) and immunocompetent C57BL/KaLwRij mice (4- to 6-week-old) were purchased from Harlan CPB (Horst, The Netherlands). For subcutaneous engraftment mice were injected with 5×10^6 5TGM1 cells subcutaneously and blindly randomized to experimental and control groups. Serial caliper measurements of perpendicular diameters were used to calculate tumor volume using the following formula: (shortest diameter)^2 × (longest diameter) × 0.52. All VSV(Δ51)-NIS treatment began after development of measurable tumors on day 7 (tumor measurements averaged 100 mm^3). Two doses of VSV(Δ51)-NIS were administered either intratumorally or intravenously on days 8 and 9 after cell implantation while the control group received phosphate-buffered saline (PBS; pH 7.4,

intratumorally) or VSV(Δ51)-GFP (intratumorally). The virus dose was 5×10^7 $TCID_{50}$/mouse/dose/0.1 mL for bg/nu/xid and 2.5×10^8 $TCID_{50}$/mouse/dose/0.1 mL for C57BL/KaLwRij mice. In radiovirotherapy experiment, ^{131}I (1 mCi/37 MBq) was administered intraperitoneally on day 10 after tumor implantation in specific groups. Mice were observed daily for signs of toxicity and weighed weekly. Animals were killed by CO_2 asphyxiation if the tumors became necrotic or grew to more that 10% of the mouse's weight. In the orthotopic 5TGM1 myeloma model, VSV(Δ51)-NIS (2.5×10^8 $TCID_{50}$/mouse/dose/0.1 mL) was administered intravenously on days 12 and 13 after intravenous injection of 5×10^6 5TGM1 cells (myeloma burden is approximately 30% in bone marrow).[31] ^{131}I was administered intraperitoneally on day 14. Myeloma paraprotein (IgG2b) levels were measured on days 12 and 29 days, respectively, after cell engraftment as described before.[31]

In a separate experiment, bg/nu/xid mice (n = 6) were killed on days 1 and 3 after virus infusion into the tail vein, tumors were harvested aseptically, and weighed. Tumors were then mechanically minced using frosted glass slides. Cellular debris was removed by low-speed centrifugation and virus titers were determined by limiting dilution on Vero cells. For toxicity studies, bg/nu/xid mice (n = 5/group) were injected with 0.2 mL PBS containing VSV-GFP, VSV(Δ51)-NIS, or VSV(Δ51)-GFP via tail vein injection. Mice were monitored for weight loss, liver or kidney damage, and signs of neurotoxicity such as huddling behavior, respiratory distress, and hind limb paralysis.

Histology and immunohistochemical staining

The bg/nu/xid mice were killed on days 1 and 4 (n = 4/group/time point) after virus administration, and their tumors were fixed in 4% formaldehyde overnight and paraffin-embedded. Serial sections (4 μm) were used for either hematoxylin and eosin staining or immunochemistry using polyclonal rabbit antibodies against VSV glycoprotein-G (provided by Dr John C. Bell, University of Ottawa, Canada). Other reagents were from a Vecastain antirabbit kit (Vector Laboratories, Burlingame, CA). Endogenous peroxidase activity was blocked by incubating with 3% H_2O_2 followed by blocking of nonspecific epitopes with normal goat serum. Sections were incubated with anti–VSV-G antibody (1:5000, 1 hour), followed by antirabbit biotinylated secondary antibody. The avidin:biotinylated enzyme complex was added and the antigen was localized by incubation with 3,3-diaminobenzidine. Sections were counterstained with hematoxylin.

^{123}I in vivo imaging studies

^{123}I animal imaging was performed on days 1 and 4 after VSV(Δ51)-NIS infection using a high-resolution micro-single photon emission computed tomography/computed tomography system (X-SPECT; Gamma Medica Ideas, Northridge, CA). Because of the large sample sizes, planar imaging only was performed. Image acquisitions were obtained 3 hours after intraperitoneal injection of ^{123}I (.5 mCi/18.5 MBq) using a low-energy, high-resolution parallel-hole collimator with a 12.5-cm field of view. Image acquisition time was 5 minutes with a 159 KeV energy (window ± 10%).

Quantitation of intratumoral radioisotope uptake was performed using a region-of-interest image analysis method previously described and validated.[32] PMOD Biomedical Image Quantification and Kinetic Modeling Software (PMOD Technologies, Zurich, Switzerland) was used for image analysis. All planar images were adjusted for equal image intensity. Corresponding total intratumoral pixel counts were converted to activity using an equation derived from previously scanning a ^{123}I standard containing a known amount of radioactivity (data not shown). Background uptake was measured and corrected for by region-of-interest image analysis of the normal opposite flank tissue and subtracted from intratumoral activity measurements obtained by region-of-interest image analysis of the tumor uptake. Whole-body activity (injected dose) in each of the mice was determined by measuring activity in the syringe in a National Institute of Standards and Technology–calibrated dose calibrator before and after injection. Percent of injected dose (%ID) in the tumor was calculated by dividing intratumoral radioactivity (corrected for background) by whole-body activity (corrected for decay and time of imaging). The calculated radioiodine uptake in the VSV(Δ51)-NIS–positive tumor is considered specific for NIS gene expression. The %ID in groups receiving PBS and VSV(Δ51)-NIS either intratumorally or intravenously were compared between days 1 and 4 to determine the optimum day for acquiring tumor-specific signal.

The absorbed radiation dose estimates in tumors were calculated by applying the Medical Internal Radiation Dose concept. For ^{123}I, Petrich et al[33] reported an effective half-life (which includes both the biologic turnover of iodine and physical radionuclide decay) of 6.5 hours. The biologic half-life (which represents the biologic turnover of iodine in the lesion) of radioactive iodine was thus calculated as 12.8 hours using the following equation: 1/T(Effective) = 1/T(Physical) + 1/T(Biological). The effective half-life for ^{131}I was calculated as 12 hours. T(Physical) was taken as 13.2 hours and 192 hours for ^{123}I and ^{131}I, respectively. The tumor dose (Gy/MBq) for ^{131}I was calculated based on in vivo uptake data of ^{123}I. The radiation dose from ^{131}I in a tumor was calculated as Dose = $C_o \times 1.443 \times T(Effective) \times S$, where C_o is the peak activity or count density, T(Effective) is the effective half-life (in hours), and S is the radiation dose per cumulated activity in the tissue.[34]

Statistical analyses

The GraphPad Prizm 4.0 program (GraphPad Software, San Diego, CA) was used for data handling, analysis, and graphic representation. Survival curves were plotted according to the Kaplan-Meier method and survival function across treatment groups was compared using log-rank test analyses.

Results

In vitro characterization of VSV(Δ51)-NIS

VSV(Δ51)-NIS was generated by cloning human NIS cDNA as an additional transcription unit between the G and L sequences of the VSV genome (Figure 1). The oncolytic activity of VSV(Δ51)-NIS was ascertained in 6 different myeloma cell lines of human and mouse origin. Cells were either mock-infected or infected with VSV(Δ51)-NIS at an MOI of 1.0, and cell viability was assessed by methyl-thiazol-tetrazolium (MTT) assay (Figure 2A). At 48 hours after infection, the percentage viability was less than 20% for all myeloma cell lines. Under similar conditions, normal mouse stromal cell line (SR-4987) and human skin fibroblasts showed minimal cell death with more than 80% cells alive at 48 hours after infection. Studies were extended to primary bone marrow samples from 3 myeloma patients. Each sample was sorted for $CD138^+$ (myeloma cell) and $CD138^-$ (normal cells) fraction, infected with VSV(Δ51)-NIS at MOI of 1.0, and assayed at 48 hours after infection. Cell viability of mock-treated $CD138^+$ and $CD138^-$ cells was used to calculate percent cell viability at 48 hours after VSV(Δ51)-NIS infection. Specific killing of $CD138^+$ myeloma cells (78%-84%) was noted (Figure 2B), whereas the $CD138^-$ cells were resistant to VSV(Δ51)-NIS–mediated cytolysis. We conclude that VSV(Δ51)-NIS efficiently and specifically replicates in and kills the myeloma cells.

One-step growth curves were performed to assess the growth kinetics and maximum virus yields of VSV(Δ51)-NIS in 5TGM1 cells (Figure 2C). The growth curves were compared with those of VSV(Δ51)-GFP.[26] At 24 hours, the progeny virus titers for VSV(Δ51)-

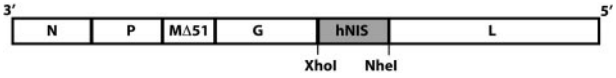

Figure 1. Schematic representation of VSV(Δ51)-NIS. The genes in the VSV(Δ51)-NIS cDNA are illustrated in 3′ to 5′ orientation. The hNIS cDNA was cloned downstream of G in the VSV(Δ51) vector using *Xho*I and *Nhe* I restriction sites. N indicates nucleocapsid protein; P, phosphoprotein; M, matrix protein; G, glycoprotein, and L, polymerase protein.

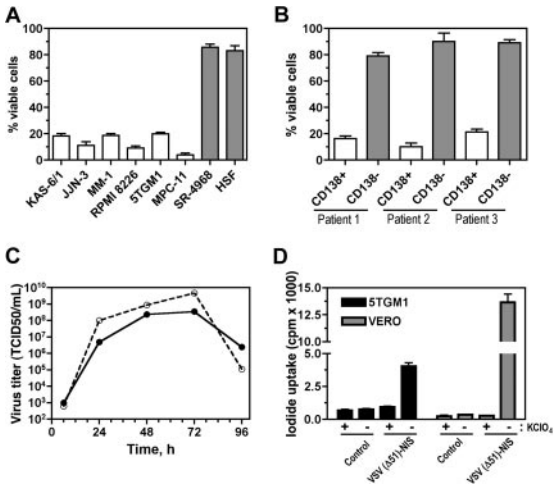

Figure 2. VSV(Δ51)-NIS virus has in vitro antimyeloma activity and VSV(Δ51)-NIS–infected cells can concentrate radioactive iodine. For cytotoxicity studies (A,B) cells were mock-infected or infected with VSV(Δ51)-NIS (MOI = 1.0) for 30 minutes at 37°C and MTT assay was performed 48 hours after infection. Experiments were performed in triplicate and cell death is expressed as relative percentage viability compared with untreated control. Bars represent mean plus or minus a SEM. (A) Cytotoxicity of VSV(Δ51)-NIS on myeloma cell lines (human and mouse), a mouse bone marrow stromal cell line (SR-4987), or human skin fibroblasts. (B) Specific cytotoxicity of VSV(Δ51)-NIS on primary CD138-positive myeloma cells versus CD138-negative normal bone marrow progenitor cells. (C) One-step growth curves for VSV(Δ51)-NIS (●) and VSV(Δ51)-GFP (Y) in 5TGM1 cells. Cells were infected with VSV(Δ51)-NIS (MOI = 1.0) for 30 minutes at 37°C, supernatants were harvested at various time points, and virus titers ($TCID_{50}$/mL) were determined on Vero cells. (D) In vitro $Na^{125}I$ uptake in 5TGM1 or Vero cells infected with VSV(Δ51)-NIS, with or without $KClO_4$. The data are presented as cpm per 10^5 cells. Experiments were performed in triplicate (mean ± SEM) and are representative of 3 independent experiments.

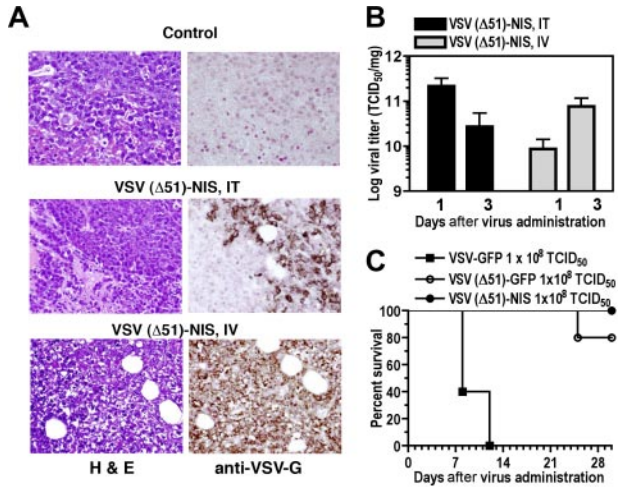

Figure 3. VSV(Δ51)-NIS replicates in subcutaneous 5TGM1 tumors. (A) Histologic analysis and immunohistochemical staining for VSV-G antigen of representative sections of 5TGM1 myeloma tumors 4 days after initiation of therapy for groups receiving no virus or VSV(Δ51)-NIS (IT or IV). Paraffin-embedded tissues were sectioned at 4-μm thickness and incubated with polyclonal anti-VSV-G antibody, which was detected with biotinylated antirabbit secondary antibody and the avidin: biotin complexing system. Sections were counterstained with hematoxylin and viewed with an Olympus BX45 microscope (Olympus, Center Valley, PA) at 40×/0.9 NA magnification. (B) 5TGM1 tumors were treated with VSV(Δ51)-NIS IT or IV, excised on days 1 and 3 after therapy, and viral titers determined by Vero cell titration. The data are expressed as log $TCID_{50}$/mg of tumor and are averaged for 3 tumors/time point. (C) Tumor-free bg/nu/xid mice received a single intravenous administration of 10^8 $TCID_{50}$ of VSV-GFP, VSV(Δ51)-NIS, or VSV(Δ51)-GFP, and were monitored for toxicity and survival (n = 5/group). Experiments were performed in triplicate (mean ± SEM).

GFP and VSV(Δ51)-NIS were 10^8 and 5×10^6 $TCID_{50}$/mL, respectively. Both viruses showed maximum virus yields at 72 hours with titers for VSV(Δ51)-GFP and VSV(Δ51)-NIS of 4.7×10^9 and 3.5×10^8 $TCID_{50}$/mL, respectively. These data show that VSV(Δ51)-NIS replicates slower than VSV(Δ51)-GFP in 5TGM1 cells.

To study if the virally expressed NIS protein was functional in VSV(Δ51)-NIS infected cells, in vitro iodide uptake assays were performed as described before.[20] Compared with mock-infected cells, iodide accumulation in 5TGM1 and Vero cells was 4.3-fold and 38.8-fold higher, respectively (Figure 2D). These uptake studies show proof of virus-driven NIS protein expression and its proper targeting to the plasma membrane.

In vivo characterization of VSV(Δ51)-NIS

Immunocompromised mice engrafted with subcutaneous 5TGM1 myeloma tumors were treated with VSV(Δ51)-NIS, then monitored for intratumoral virus replication and tumor response. On day 4 after intravenous or intratumoral administration of VSV(Δ51)-NIS, strong VSV-G–specific immunoreactivity was seen in the tumors of virus-treated groups while the control tumors scored negative (Figure 3A). Both intratumoral and intravenous administration resulted in high viral titers in the subcutaneous tumors on days 1 and 3 after virus administration (Figure 3B). Interestingly, intratumoral administration of VSV(Δ51)-NIS led to higher intratumoral viral titers on day 1 compared with day 3 (2.2×10^{11} and 2.7×10^{10} $TCID_{50}$/mg on days 1 and 3, respectively). Conversely, for the group receiving intravenous VSV(Δ51)-NIS, the viral titers were higher on day 3 (8.7×10^9 to 7.7×10^{10} $TCID_{50}$/mg for days 1 and 3, respectively). For both intratumoral and intravenous groups, a 100-fold lower virus titer was observed by day 7 (data not shown).

To determine the safety of intravenous administration of VSV(Δ51)-NIS in bg/nu/xid mice, toxicity studies were performed in animals (n = 5/group) treated with VSV-GFP, VSV(Δ51)-GFP, or VSV(Δ51)-NIS (2 doses of 5×10^7 $TCID_{50}$/dose). By day 12 after virus administration, all of the mice receiving VSV-GFP were dead, with signs characteristic of VSV-induced neurotoxicity.[26,29,35] Mice receiving VSV(Δ51)-NIS showed no signs of VSV-induced neurotoxicity even 2 months after virus treatment. In the VSV(Δ51)-GFP group, one animal died on day 24 after virus administration for unknown reasons. A detailed necropsy was not performed but the brain was excised, homogenized, and incubated with Vero cells, and no virus-induced cytopathic effect was detected at 72 hours (data not shown). These toxicity data show that VSV(Δ51)-NIS can be safely administered by the intravenous route even in immunocompromised bg/nu/xid mice at a dose of 10^8 $TCID_{50}$ (Figure 3C).

To evaluate the potential of *NIS* as a reporter gene for noninvasive localization of virus infected cells, planar gamma camera scintigraphy was performed to determine the biodistribution of ^{123}I in VSV(Δ51)-NIS treated bg/nu/xid mice. Whole-body images of the virus-treated animals showed definite iodide uptake by the VSV(Δ51)-NIS infected tumors, whereas no iodine signal was seen in the tumors of control mice injected with PBS (Figure 4A) or with VSV(Δ51)-GFP (data not shown). Quantitation of intratumoral radioisotope uptake showed that the percentage injected radioiodine dose (%ID) taken up by these tumors was 0, 4.1, or 7.0 for the control, intratumoral, and intravenous VSV(Δ51)-NIS–treated mice, respectively (Figure 4A). Iodide accumulation was also seen in the thyroid and the stomach, organs known to express endogenous NIS, and in the bladder as a result of iodide excretion via the kidneys.

To determine whether analysis of planar gamma camera images could be used to monitor intratumoral virus propagation, mice were

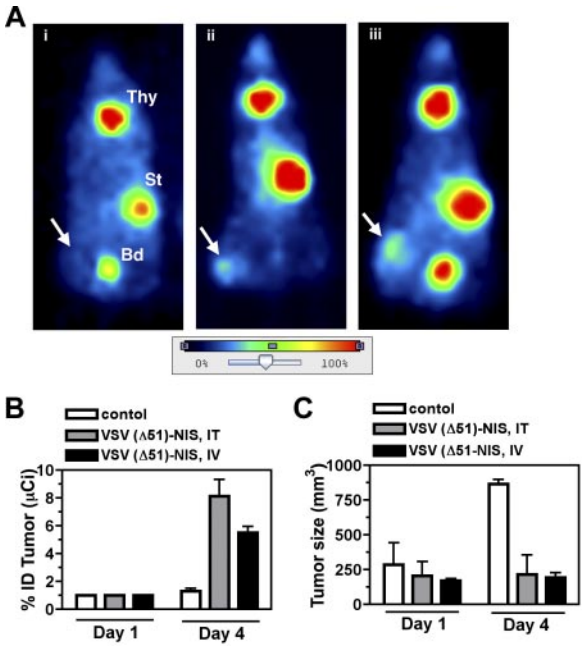

Figure 4. Imaging, dosimetric, and oncolytic activity of VSV(Δ51)-NIS. (A) Representative planar images of VSV(Δ51)-NIS–infected, tumor-bearing mice obtained 3 hours after intraperitoneal injection of ^{123}I 1 day after mock (PBS, intratumoral) or VSV(Δ51)-NIS injections (5×10^7 $TCID_{50}$/dose, 2 doses given days −1 and 0). Radioisotope uptake is seen in the salivary glands, thyroid gland (Thy), and stomach (St), with excreted radioisotope visible in the bladder (Bd). No increased uptake is seen in the subcutaneous flank tumor of (i) control mouse, whereas increased intratumoral radioisotope uptake is demonstrated in mice treated (ii) intratumorally or (iii) intravenously with VSV(Δ51)-NIS. Arrows indicate tumor locations. The color bar (image intensity scale) demonstrates the range of uptake intensities, with 100% representing the strongest signal in the image. Planar images were acquired using a Gamma Medica X-SPECT imaging system (Gamma Medica, Northridge, CA). Images were analyzed and processed using PMOD Biomedical Image Quantification and Kinetic Modeling software version 2.75 (PMOD Technologies) and Adobe Photoshop version 7.0 (Adobe Systems, San Jose, CA). (B) Serial planar images of subcutaneous myeloma tumors were acquired on days 1 and 4 after administration of VSV(Δ51)-NIS and %ID taken up by the tumor was calculated (n = 4/group). (C) The growth of subcutaneous myeloma tumors was tested by measuring tumor volumes on days 1 and 4 (n = 4/group). Bars indicate SE.

serially imaged on days 1 and 4 after VSV(Δ51)-NIS administration and tumor specific activity at each of these time points was calculated and expressed as %ID (Figure 4B). The %ID for all groups at day 0 was set to 1 and the fold-increase was calculated at day 4 (n = 4/group). On day 4, the fold-increase in %ID in the tumors of mice receiving VSV(Δ51)-NIS by intratumoral or intravenous routes was 8.1 (± 2.4) and 5.5 (± 0.9), respectively. The control group receiving PBS showed a nonsignificant change from 1 to 1.3 (± 0.4) in tumor radioiodine uptake. When tumor sizes were compared between the virus-treated and control groups, the average tumor sizes for the groups receiving VSV(Δ51)-NIS did not change significantly from day 1 to day 4. However, in the control group the untreated tumors tripled in size between days 1 and 4. (Figure 4C).

In vivo virotherapy of myeloma tumors with VSV(Δ51)-NIS

To evaluate the in vivo oncolytic potency of the VSV(Δ51)-NIS virus, bg/nu/xid mice bearing subcutaneous 5TGM1 tumors (n = 10/group) were given 2 doses of VSV(Δ51)-NIS (5×10^7 $TCID_{50}$/dose) by IT or IV injection, whereas control mice (n = 5) received PBS by the same route. In control mice, rapid tumor growth was observed whereas tumor growth was arrested in mice treated with VSV(Δ51)-NIS, IT or IV (Figure 5A). The average survival time for control animals receiving PBS was 22 days after tumor

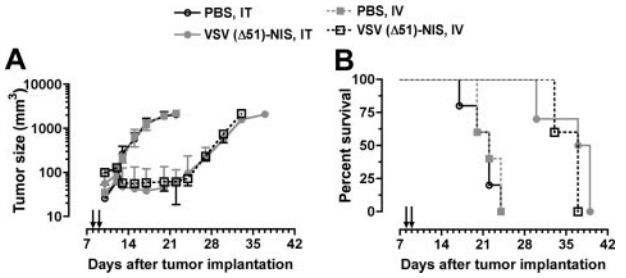

Figure 5. VSV(Δ51)-NIS controls the growth of myeloma tumors in bg/nu/xid mice. Mice bearing subcutaneous myeloma tumors (mean volume 100 mm^3) were treated with VSV(Δ51)-NIS (2 doses of 5×10^7 $TCID_{50}$/dose) and monitored for (A) tumor growth. Points, mean tumor volumes (n = 10 for test groups and n = 5 for the control groups); bars indicate SE. (B) Kaplan-Meier survival curves of mice treated with saline or VSV(Δ51)-NIS (intratumorally or intravenously). Arrows indicate virus injections.

engraftment, whereas the average survival times for mice receiving VSV(Δ51)-NIS (intratumorally or intravenously) were 38 days ($P < .001$) or 37 days ($P < .001$), respectively. These studies show that, in the absence of a functional immune system, VSV(Δ51)-NIS has oncolytic activity against myeloma tumors in vivo.

Dosimetric calculations

To determine whether a therapeutic effect might be achieved by combining VSV(Δ51)-NIS with the radionuclide ^{131}I, in vivo imaging studies with ^{123}I were performed and the data were used for dosimetry calculations (Table 1). Assuming a total ^{131}I dose of 1 mCi, predicted tumor-absorbed doses were estimated to be 18.4 (± 5.9) Gy (n = 20, $P = 0.03$) and 11.6 (± 2.3) Gy (n = 20, $P = .02$), with VSV(Δ51)-NIS given IT or IV, respectively, on day 1 after virus administration. The predicted tumor absorbed dose for the control group was 4.2 (± 2.1) Gy. These results illustrated how ^{123}I biodistribution data can be used for dosimetric calculations to estimate potential tumor absorbed doses for radiovirotherapy studies and suggested that the administration of ^{131}I could enhance the therapeutic efficacy of VSV(Δ51)-NIS therapy.

VSV(Δ51)-NIS for radiovirotherapy of subcutaneous and orthotopic myeloma in immunocompetent mice

To determine whether administration of ^{131}I could enhance the therapeutic efficacy of VSV(Δ51)-NIS therapy, we used the syngeneic immunocompetent 5TGM1 murine myeloma model (Figure 6). For these experiments the total virus dose was increased from 10^8 $TCID_{50}$ to 5×10^8 $TCID_{50}$ because VSV particles can be rapidly inactivated by the host immune system.[18]

Initial studies were conducted in immunocompetent C57BL/KaLwRij mice bearing subcutaneous 5TGM1 tumors. The tumors

Table 1. Dosimetric calculations (MIRD) for ^{131}I

	Intratumoral injections		Intravenous injections	
	PBS*	VSV (Δ51)-NIS†	PBS*	VSV (Δ51)-NIS†
Tumor volume, mm^3	180	170	190	120
Injected activity, MBq ^{123}I	10.5	10.4	10.3	11.0
Tumor activity, MBq ^{123}I	0.1	0.6	0.1	0.6
Tumor dose, Gy ^{131}I	4.2	18.4	4.1	11.6

Dosimetric calculations were based on imaging studies (with ^{123}I) performed on day 1 after virus administration in mice bearing subcutaneous 5TGM1 myeloma tumors. Mice were given PBS or VSV (Δ51)-NIS (5×10^7 $TCID_{50}$/dose, 2 doses given 24 hours apart) by intratumoral or intravenous routes.

MIRD indicates medical internal radiation dosimetry.

*N=10.

†N=20.

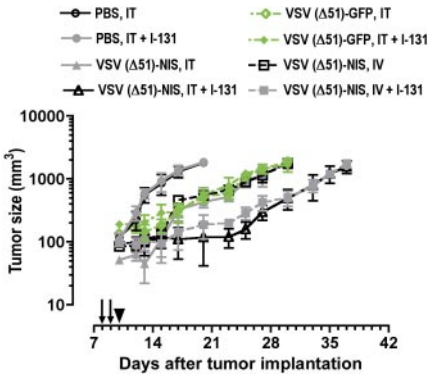

Figure 6. Radiovirotherapy of myeloma tumors in syngeneic, immunocompetent mice. C57BL6/KaLwRij mice with established subcutaneous myeloma tumors were treated with VSV(Δ51)-NIS or VSV(Δ51)-GFP (2 doses of 2.5×10^8 $TCID_{50}$/dose) without or with ^{131}I (1 mCi/mouse intraperitoneally 24 hours after virus administration) and tumor volumes are plotted against days after treatment. Arrows indicate virus injections; arrowhead, ^{131}I injection; points, mean; bars, SE.

progressed rapidly in control mice (Figure 6, Table 2). With intratumoral and intravenous injections of VSV(Δ51)-NIS or VSV(Δ51)-GFP, tumor growth was suppressed until day 5 after therapy, after which the tumors grew rapidly. In mice receiving VSV(Δ51)-NIS followed by a therapeutic dose of ^{131}I, the growth of tumors was arrested until day 15 after therapy. ^{131}I significantly enhanced the antitumor potency of VSV(Δ51)-NIS but had no effect on the antitumor potency of VSV(Δ51)-GFP. Tumor sizes were compared between the various groups on day 20 after tumor implantation (Table 2). Kaplan-Meier curves showed median survivals of animals treated intravenously with VSV(Δ51)-NIS were prolonged significantly by the addition of ^{131}I, from 28.5 to 35 days in the group that was treated intravenously ($P = .02$). These data show that VSV(Δ51)-NIS is able to arrest tumor growth in immune competent mice and exhibits increased potency when combined with ^{131}I.

We next evaluated the potential synergy of VSV(Δ51)-NIS and ^{131}I in immunocompetent C57BL/KaLwRij mice bearing orthotopic 5TGM1 tumors. Single-agent VSV(Δ51)-NIS therapy prolonged survival from 30 to 33 days (Figure 7A). Radiovirotherapy prolonged the median survival to 38.5 days ($P = .001$, compared with ^{131}I control ($P = .041$) compared with single-agent VSV(Δ51)-NIS (Figure 7A). Serum paraprotein levels were measured to monitor myeloma progression in these mice (Figure 7B). On day 12 after myeloma engraftment, the paraprotein levels were comparable between groups (n = 4/group) and ranged from 3.2 to 3.9 g/L (data not shown). On day 29, at which point most of the control mice injected with PBS or ^{131}I showed terminal paraplegia, the IgG2b levels were 7.5 (± 0.9) g/L, 6.4 (± 0.5) g/L, and 4.9 (± 0.6) g/L, respectively, for the mice injected with PBS, VSV(Δ51)-NIS, or VSV(Δ51)-NIS plus ^{131}I. Thus, the VSV(Δ51)-NIS virus was able to inhibit myeloma progression in vivo and this inhibitory effect was more pronounced with ^{131}I.

Discussion

Here we report for the first time a novel recombinant virus, VSV(Δ51)-NIS, and demonstrate that it can be used for its oncolytic and imaging properties in multiple myeloma.

Pathogenic strains of VSV generally cause mild benign infections in humans.[36] However, similar to other RNA viruses, VSV shows neurotropism if given direct access to brain tissue. In immunodeficient mice, VSV infections are associated with fatal meningoencephalitis,[37] whereas immunocompetent mice can clear the virus before neurotoxicity is seen, at least at lower challenge doses. Efficient viral clearance is dependent on activation of innate and adaptive immune responses. Wild-type strains of VSV are poor inducers of IFN-α/β[38] because the VSV matrix (M) protein blocks expression of interferon stimulated genes by binding to a nuclear RNA export factor RAE1 (MRNP41).[39] VSVs carrying certain mutation(s) or a deletion in the M protein [eg, M51R,[35,40] V221F, S226R, or Δ51[26]] cannot suppress the cellular interferon response, and therefore grow poorly in normal tissues showing greatly reduced neurotoxicity but little reduction in their tumor-killing ability.[23,33,43] Other approaches to increase the therapeutic index of VSV include the generation of recombinant viruses engineered to express the mouse or human IFN-β genes[29] or prophylactic IFN-α treatment before challenge with wild-type VSV.[41,42] Our in vivo studies show that 2 doses of VSV(Δ51)-NIS (5×10^7 $TCID_{50}$/dose) are well tolerated by bg/nu/xid mice.

The concept of radiovirotherapy for multiple myeloma was originally established using a recombinant measles virus coding for NIS (MV-NIS),[16] which is currently being evaluated in phase I clinical trials at Mayo Clinic. Compared with MV, VSV has a very rapid replication cycle time of 8 to 12 hours in permissive tumor cells.[43] In vitro studies using various cancer cell lines have shown complete killing by 48 to 96 hours after infection with VSV strains mutated in the matrix protein.[26,35] Our in vitro studies show that VSV(Δ51)-NIS has slower growth compared with VSV-GFP. This may allow a longer period of expression of the NIS transgene in the plasma membrane prior to virus induced killing of the infected cells, thus enabling active concentration of iodide ions before the cell dies.[44]

Because mouse cells lack MV receptors, in vivo studies of MV-NIS were conducted in SCID mice bearing human myeloma

Table 2. Average tumor volumes (day 20 after tumor implantation) in immunocompetent mice bearing subcutaneous 5TGM1 myeloma tumors after administration of recombinant VSV without or with ^{131}I

Treatment	Mice/group	Average tumor volume, mm^3 plus or minus SD	95% CI of mean (mm^3)	
			Lower	Upper
PBS, intratumorally	4	1796.0 ± 231.9	1427.0	2165
PBS, intratumorally + ^{131}I	4	1809.0 ± 186.2	1512.1	2105.0
VSV (Δ51)-NIS, ITintratumorally	6	421.3 ± 100.2	316.2	526.4
VSV (Δ51)-NIS, intratumorally + ^{131}I	6	129.0 ± 63.3	62.6	195.4
VSV (Δ51)-NIS, intravenously	6	558.0 ± 114.2	438.1	677.9
VSV (Δ51)-NIS, intravenously + ^{131}I	6	204.0 ± 110.5	88.1	319.9
VSV (Δ51)-GFP, intratumorally	4	494.5 ± 166.2	230.1	758.9
VSV (Δ51)-GFP, intratumorally + ^{131}I	4	524.5 ± 156.5	275.4	773.6

Virus was administered on days 12 and 13 (intratumorally or intravenously) and ^{131}I (1 mCi) was given intraperitoneally on day 14 after tumor-cell inoculation.

Table 3. Median survival of immunocompetent mice bearing subcutaneous myeloma tumors after administration of recombinant VSV without or with ^{131}I

Treatment	Mice per group	Median survival, d	*P* compared with PBS	*P* compared with Respective rVSV construct
PBS	4	20.0	—	—
PBS + ^{131}I	4	20.0	NS	—
VSV(Δ51)-NIS, intratumorally	6	30.0	.002	.213
VSV(Δ51)-NIS, intratumorally + ^{131}I	6	32.0	.002	—
VSV(Δ51)-NIS, intravenously	6	28.5	.002	.018
VSV(Δ51)-NIS, intravenously + ^{131}I	6	35.0	.002	—
VSV(Δ51)-GFP, intratumorally	4	28.5	.01	NS
VSV(Δ51)-GFP, intratumorally + ^{131}I	4	28.5	.01	—

rVSV was administered on days 12 and 13 after tumor cell inoculation. ^{131}I was given intraperitoneally on day 14. Kaplan-Meier survival curves were drawn.

NS indicates not significant; —, not applicable.

xenografts.[20] In contrast to MV receptors, VSV receptors are ubiquitously expressed on mouse and human cells. VSV(Δ51)-NIS was therefore studied in the murine 5TGM1 myelomamodel. 5TGM1 provides a valuable orthotopic model of multiple myeloma, allowing the study of myeloma cell growth and survival in a normal murine bone marrow microenvironment.[31,45,46] In addition to intratumoral injection, we studied systemic administration of VSV(Δ51)-NIS because myeloma is a disseminated malignancy and it is essential to develop therapeutic agents that can be administered systemically. Studies by other investigators have shown that systemic administration of VSV in mouse models can target both primary and metastatic tumors.[26,29,35,47] Our in vivo studies show that intravenous administration of VSV(Δ51)-NIS resulted in infection and viral spread in subcutaneous myeloma tumors.

NIS imaging offers a convenient approach to noninvasively confirm correct localization of virus- or plasmid-encoded NIS gene expression before proceeding to ^{131}I therapy.[8] Numerous factors can influence NIS expression and hence the intensity of the NIS-mediated radioiodine image. Variable susceptibility of tumor cells to viral transduction and virus-mediated killing, variable rates of intratumoral virus propagation, variable tumor sizes and tumor injection techniques, and variable rates of tumor regression are just a few of the factors that influence the image signal intensity after treatment with an oncolytic virus expressing NIS. We performed serial imaging on mice bearing subcutaneous myeloma tumors on days 1 and 4 after VSV(Δ51)-NIS administration. A specific signal was detected in the myeloma tumors after injection of VSV(Δ51)-NIS but not in the control groups, allowing us to attribute the tumor specific signal to virus-driven expression of the NIS gene.

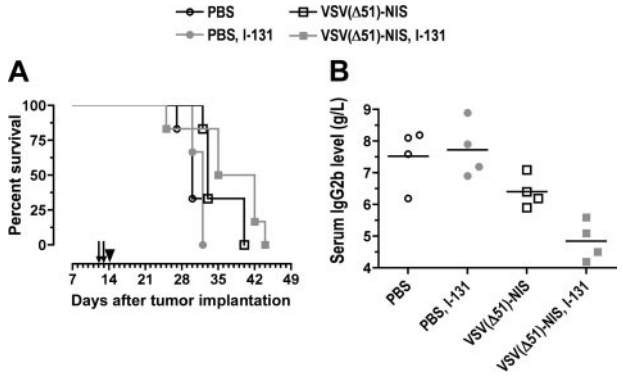

Figure 7. Radiovirotherapy of orthtopic myeloma tumors in syngeneic, immunocompetent mice. C57BL6/KaLwRij mice with disseminated myeloma were treated with VSV(Δ51)-NIS (2 doses of 2.5×10^8 $TCID_{50}$/dose) without or with ^{131}I (1 mCi/mouse intraperitoneally 24 hours after virus administration). (A) Median survival of mice is shown as Kaplan-Meier plots. Arrows indicate virus injections and arrowhead indicate ^{131}I injection. (B) Myeloma burden of various cohorts was determined by measuring serum IgG2b levels on day 29 after tumor engraftment (n = 4 per group, average values are shown by line).

Several preclinical studies have demonstrated ablative effects of ^{131}I in tumor xenografts.[12,15,48-53] Dosimetry calculations predicted that we would achieve cumulative radiation-absorbed doses to the VSV(Δ51)-NIS–infected myeloma tumors of approximately 11 to 18 Gy after a therapeutic dose of 1 mCi of ^{131}I-iodide. Beta particle crossfire is an important mechanism contributing to the antitumor activity of intratumoral ^{131}I. Each beta particle emitted by ^{131}I deposits its energy within a local area of 2 to 3 mm from the point of decay such that a field of beta particle crossfire can exist only in a large tumor with multiple foci of radioiodine accumulation. Three-dimensional spheroids have been thus used with NIS radioiodide approach to assess therapeutic efficacy.[54,55] Tumor deposits in orthotopic myeloma models are typically very small (up to 2-mm diameter) even when the disease is far advanced. For this reason we focused our studies initially on mice bearing subcutaneous myeloma tumors with diameters of approximately 5mm. Because bg/nu/xid mice are hypersensitive to ionizing radiation and therefore unsuitable for radiovirotherapy studies, we used immunocompetent C57BL6/KaLwRij mice bearing subcutaneous 5TGM1 tumors. The results obtained in this model demonstrated the superior potency of radiovirotherapy compared with single-agent VSV(Δ51)-NIS. Despite our reservations because of the small size of tumor deposits in orthotopic myeloma models, we next extended our radiovirotherapy studies to the 5TGM1 syngeneic orthotopic murine myeloma model.[31] VSV(Δ51)-NIS alone did not significantly prolong survival in this model unless it was followed by treatment with ^{131}I. Several studies have shown that VSV provokes the production of neutralizing antibodies, and we are conducting studies to determine whether this will lead to attenuated antitumor potency in this model.[56] We are also testing strategies to suppress the anti-VSV immune response and to evade it by delivering the VSV inside infected cell carriers.[57]

In conclusion, we have generated and characterized a novel oncolytic VSV encoding the NIS gene. Our results show that this agent can be safely administered by the intravenous route and has strong oncolytic activity against myeloma tumors. The NIS transgene can be used to image VSV(Δ51)-NIS–infected myeloma tumors by planar scintigraphy. Therapeutic potency was enhanced by combining VSV(Δ51)-NIS with ^{131}I in radiovirotherapy studies. VSV(Δ51)-NIS is a promising new experimental agent that should be further developed for the treatment of multiple myeloma.

Acknowledgments

The authors thank the Histology Core at Mayo Clinic, Scottsdale, AZ. The authors also acknowledge Tracy Decklever, Department of Radiology, Mayo Clinic, for helping in the acquisition of planar images.

This work was supported by grants from National Institutes of Health (NIH; CA100634-02 and HL66958-3P4). J.B. is supported by a Terry Fox Program Project grant, and A.P. is supported by an

Ontario Graduate Scholarship in Science and Technology (OGSST) studentship.

Authorship

Contribution: A.G. designed the study, conducted in vitro and in vivo experiments, analyzed the data, and wrote the manuscript. S.K.C. performed image analysis for calculating percent of injected dose of iodine-123 to the tumor. K.L.C. performed dosimetric analysis for iodine-131. S.G. contributed to animal experiments. S.N. conducted in vitro and in vivo experiments and assisted with analysis of data. A.T.P. constructed and rescued VSV-NIS virus. J.C.B. provided anti-VSV-G antibodies, oversaw generation of VSV-NIS virus, and provided expertise about VSV. S.J.R. conceptualized the study, oversaw in vivo studies, and cowrote the manuscript.

Conflict-of-interest disclosure: The authors declare no competing financial interests.

Correspondence: Stephen J. Russell, Mayo Clinic, Guggenheim 1833, 200 First St. SW, Rochester, MN 55905; e-mail: sjr@mayo.edu.

References

1. Kyle RA. Multiple myeloma: an odyssey of discovery. Br J Haematol. 2000;111:1035-1044.
2. Kyle RA. Current therapy of multiple myeloma. Intern Med. 2002;41:175-180.
3. Jemal A, Murray T, Ward E, et al. Cancer statistics, 2005. CA Cancer J Clin. 2005;55:10-30.
4. Glück S, Van Dyk J, Messner HA. Radiosensitivity of human clonogenic myeloma cells and normal bone marrow precursors: effect of different dose rates and fractionation. Int J Radiat Oncol Biol Phys. 1994;28:877-882.
5. Goel A, Dispenzieri A, Greipp PR, Witzig TE, Mesa RA, Russell SJ. PS-341-mediated selective targeting of multiple myeloma cells by synergistic increase in ionizing radiation-induced apoptosis. Exp Hematol. 2005;33:784-795.
6. Björkstrand B. European Group for Blood and Marrow Transplantation Registry studies in multiple myeloma. Semin Hematol. 2001;38:219-225.
7. Moreau P, Facon T, Attal M, et al. Comparison of 200 mg/m(2) melphalan and 8 Gy total body irradiation plus 140 mg/m(2) melphalan as conditioning regimens for peripheral blood stem cell transplantation in patients with newly diagnosed multiple myeloma: final analysis of the Intergroupe Francophone du Myelome 9502 randomized trial. Blood. 2002;99:731-735.
8. Dingli D, Russell SJ, Morris JC, 3rd. In vivo imaging and tumor therapy with the sodium iodide symporter. J Cell Biochem. 2003;90:1079-1086.
9. Dai G, Levy O, Carrasco N. Cloning and characterization of the thyroid iodide transporter. Nature. 1996;379:458-460.
10. Chung JK. Sodium iodide symporter: its role in nuclear medicine. J Nucl Med. 2002;43:1188-1200.
11. Dingli D, Diaz RM, Bergert ER, O'Connor MK, Morris JC, Russell SJ. Genetically targeted radiotherapy for multiple myeloma. Blood. 2003;102:489-496.
12. Dwyer RM, Bergert ER, O'Connor MK, Gendler SJ, Morris JC. In vivo radioiodide imaging and treatment of breast cancer xenografts after MUC1-driven expression of the sodium iodide symporter. Clin Cancer Res. 2005;11:1483-1489.
13. Hart IR. Tissue specific promoters in targeting systemically delivered gene therapy. Semin Oncol. 1996;23:154-158.
14. Kakinuma H, Bergert ER, Spitzweg C, Cheville JC, Lieber MM, Morris JC. Probasin promoter (ARR(2)PB)-driven, prostate-specific expression of the human sodium iodide symporter (h-NIS) for targeted radioiodine therapy of prostate cancer. Cancer Res. 2003;63:7840-7844.
15. Spitzweg C, O'Connor MK, Bergert ER, Tindall DJ, Young CY, Morris JC. Treatment of prostate cancer by radioiodine therapy after tissue-specific expression of the sodium iodide symporter. Cancer Res. 2000;60:6526-6530.
16. Spitzweg C, Zhang S, Bergert ER, et al. Prostate-specific antigen (PSA) promoter-driven androgen-inducible expression of sodium iodide symporter in prostate cancer cell lines. Cancer Res. 1999;59:2136-2141.
17. Bell JC, Lichty B, Stojdl D. Getting oncolytic virus therapies off the ground. Cancer Cell. 2003;4:7-11.
18. Parato KA, Senger D, Forsyth PA, Bell JC. Recent progress in the battle between oncolytic viruses and tumours. Nat Rev Cancer. 2005;5:965-976.
19. Peng KW, Ahmann GJ, Pham L, Greipp PR, Cattaneo R, Russell SJ. Systemic therapy of myeloma xenografts by an attenuated measles virus. Blood. 2001;98:2002-2007.
20. Dingli D, Peng KW, Harvey ME, et al. Image-guided radiovirotherapy for multiple myeloma using a recombinant measles virus expressing the thyroidal sodium iodide symporter. Blood. 2004;103:1641-1646.
21. Russell SJ. RNA viruses as virotherapy agents. Cancer Gene Ther. 2002;9:961-966.
22. Lichty BD, Power AT, Stojdl DF, Bell JC. Vesicular stomatitis virus: re-inventing the bullet. Trends Mol Med. 2004;10:210-216.
23. Lichty BD, Stojdl DF, Taylor RA, et al. Vesicular stomatitis virus: a potential therapeutic virus for the treatment of hematologic malignancy. Hum Gene Ther. 2004;15:821-831.
24. Balachandran S, Barber GN. Vesicular stomatitis virus (VSV) therapy of tumors. IUBMB Life. 2000;50:135-138.
25. Fernandez M, Porosnicu M, Markovic D, Barber GN. Genetically engineered vesicular stomatitis virus in gene therapy: application for treatment of malignant disease. J Virol. 2002;76:895-904.
26. Stojdl DF, Lichty BD, tenOever BR, et al. VSV strains with defects in their ability to shutdown innate immunity are potent systemic anti-cancer agents. Cancer Cell. 2003;4:263-275.
27. Radl J. Idiopathic paraproteinemia–a consequence of an age-related deficiency in the T immune system. Three-stage development–a hypothesis. Clin Immunol Immunopathol. 1979;14:251-255.
28. Lawson ND, Stillman EA, Whitt MA, Rose JK. Recombinant vesicular stomatitis viruses from DNA. Proc Natl Acad Sci U S A. 1995;92:4477-4481.
29. Obuchi M, Fernandez M, Barber GN. Development of recombinant vesicular stomatitis viruses that exploit defects in host defense to augment specific oncolytic activity. J Virol. 2003;77:8843-8856.
30. Hadac EM, Peng KW, Nakamura T, Russell SJ. Reengineering paramyxovirus tropism. Virology. 2004;329:217-225.
31. Goel A, Dispenzieri A, Geyer SM, Greiner S, Peng KW, Russell SJ. Synergistic activity of the proteasome inhibitor PS-341 with non-myeloablative 153-Sm-EDTMP skeletally targeted radiotherapy in an orthotopic model of multiple myeloma. Blood. 2006;107:4063-4070.
32. Carlson SK, Classic KL, Hadac EM, et al. In vivo quantitation of intratumoral radioisotope uptake using micro-single photon emission computed tomography/computed tomography. Mol Imaging Biol. 2006;8:324-332.
33. Petrich T, Helmeke HJ, Meyer GJ, Knapp WH, Potter E. Establishment of radioactive astatine and iodine uptake in cancer cell lines expressing the human sodium/iodide symporter. Eur J Nucl Med Mol Imaging. 2002;29:842-854.
34. Reynolds JC. Percent 131I uptake and post-therapy 131I scans: their role in the management of thyroid cancer. Thyroid. 1997;7:281-284.
35. Ebert O, Harbaran S, Shinozaki K, Woo SL. Systemic therapy of experimental breast cancer metastases by mutant vesicular stomatitis virus in immune-competent mice. Cancer Gene Ther. 2005;12:350-358.
36. Letchworth GJ, Rodriguez LL, Del cbarrera J. Vesicular stomatitis. Vet J. 1999;157:239-260.
37. Huneycutt BS, Bi Z, Aoki CJ, Reiss CS. Central neuropathogenesis of vesicular stomatitis virus infection of immunodeficient mice. J Virol. 1993;67:6698-6706.
38. Marcus PI, Rodriguez LL, Sekellick MJ. Interferon induction as a quasispecies marker of vesicular stomatitis virus populations. J Virol. 1998;72:542-549.
39. Faria PA, Chakraborty P, Levay A, et al. VSV disrupts the Rae1/mrnp41 mRNA nuclear export pathway. Mol Cell. 2005;17:93-102.
40. Desforges M, Charron J, Berard S, et al. Different host-cell shutoff strategies related to the matrix protein lead to persistence of vesicular stomatitis virus mutants on fibroblast cells. Virus Res. 2001;76:87-102.
41. Stojdl DF, Lichty B, Knowles S, et al. Exploiting tumor-specific defects in the interferon pathway with a previously unknown oncolytic virus. Nat Med. 2000;6:821-825.
42. Shinozaki K, Ebert O, Suriawinata A, Thung SN, Woo SL. Prophylactic alpha interferon treatment increases the therapeutic index of oncolytic vesicular stomatitis virus virotherapy for advanced hepatocellular carcinoma in immune-competent rats. J Virol. 2005;79:13705-13713.
43. Rose JKaW, M.A. Rhabdoviridae: the viruses and their replication.: Philadelphia: Lippincott Williams and Wilkins; 2001.
44. Eskandari S, Loo DD, Dai G, Levy O, Wright EM, Carrasco N. Thyroid Na+/I- symporter. Mechanism, stoichiometry, and specificity. J Biol Chem. 1997;272:27230-27238.
45. Dallas SL, Garrett IR, Oyajobi BO, et al. Ibandronate reduces osteolytic lesions but not tumor burden in a murine model of myeloma bone disease. Blood. 1999;93:1697-1706.
46. Turner JH, Claringbold PG, Manning LS, O'Donoghue HL, Berger JD, Glancy RJ. Radiopharmaceutical therapy of 5T33 murine myeloma by sequential treatment with samarium-153 ethylenediaminetetramethylene phosphonate, melphalan, and bone marrow transplantation. J Natl Cancer Inst. 1993;85:1508-1513.
47. Balachandran S, Porosnicu M, Barber GN. Oncolytic activity of vesicular stomatitis virus is effective against tumors exhibiting aberrant p53, Ras,

or myc function and involves the induction of apoptosis. J Virol. 2001;75:3474-3479.

48. Nakamoto Y, Saga T, Misaki T, et al. Establishment and characterization of a breast cancer cell line expressing Na+/I- symporters for radioiodide concentrator gene therapy. J Nucl Med. 2000;41:1898-1904.
49. Boland A, Ricard M, Opolon P, et al. Adenovirus-mediated transfer of the thyroid sodium/iodide symporter gene into tumors for a targeted radiotherapy. Cancer Res. 2000;60:3484-3492.
50. Spitzweg C, Dietz AB, O'Connor MK, et al. In vivo sodium iodide symporter gene therapy of prostate cancer. Gene Ther. 2001;8:1524-1531.
51. Cho JY, Shen DH, Yang W, et al. In vivo imaging and radioiodine therapy following sodium iodide symporter gene transfer in animal model of intracerebral gliomas. Gene Ther. 2002;9:1139-1145.
52. Dwyer RM, Bergert ER, O'Connor M K, Gendler SJ, Morris JC. Adenovirus-mediated and targeted expression of the sodium-iodide symporter permits in vivo radioiodide imaging and therapy of pancreatic tumors. Hum Gene Ther. 2006;17:661-668.
53. Dwyer RM, Bergert ER, O'Connor MK, Gendler SJ, Morris JC. Sodium iodide symporter-mediated radioiodide imaging and therapy of ovarian tumor xenografts in mice. Gene Ther. 2006;13:60-66.
54. Mitrofanova E, Hagan C, Qi J, Seregina T, Link C, Jr. Sodium iodide symporter/radioactive iodine system has more efficient antitumor effect in three-dimensional spheroids. Anticancer Res. 2003;23:2397-2404.
55. Mitrofanova E, Unfer R, Vahanian N, Link C. Rat sodium iodide symporter allows using lower dose of 131I for cancer therapy. Gene Ther. 2006;13:1052-1056.
56. Barber GN. Vesicular stomatitis virus as an oncolytic vector. Viral Immunol. 2004;17:516-527.
57. Power AT, Wang J, Falls TJ, et al. Carrier cell-based delivery of an oncolytic virus circumvents antiviral immunity. mol ther. 2007;15:123-130.